encit 2020

ABCM Associação Brasileira de Engenharia e Ciências Mecânicas

18th Brazilian Congress of Thermal Sciences and Engineering
November 16-20, 2020 (Online)

ENC-2020-0024
THERMAL DEVELOPMENT IN THE FLOW OF OILS IN BIFURCATIONS

Flavio Peres Amado
Universidade Estacio de Sá, Rua Eduardo Luiz Gomes, 134 - Morro do Estado, Niterói - RJ, 24020-340
e-mails: flavioam@petrobras.com.br; fpamado@live.estacio.com.br
Victor Hugo Corradi Mondaini
Alessandro Raphael Antunes
Paulo Ricardo Valentim
Nilton Paiva de Carvalho Júnior
Universidade Estacio de Sá, Rua Eduardo Luiz Gomes, 134 - Morro do Estado, Niterói - RJ, 24020-340
e-mails:vic.hugmondaini@yahoo.com.br; ricardovalentim77@gmail.com; alessandro.r.antunes@gmail.com; jnr280@hotmail.com

Abstract. *This manuscript deals with qualitative and quantitative analysis of the region of thermal development in bifurcations, where four families of oils flow, namely, biodiesels, edibles, hydraulics and lubricants. Ultimately, this reality translates into the variation in fluid viscosity and density. The flow rate used is that which induces a Reynolds Number bordering on laminar flow. CFD-type simulations were carried out in finite differences and through a commercial package. Results show that the thermal developing regions presented in the simulated universe are quite morphologically similar to the flow developing region. That is an expected fact, since the energy equation, which determines the temperature gradient, uses the velocity field in its calculations, predicted by the moment equations. The lengths of the region of interest, measured in the images generated in the simulations, did not find a good coincidence of values with the lengths calculated by correlations found in the related literature. Thus, a new correlation is proposed for the universe tested in this paper. This manuscript closes the study cycle of the flow and thermal developing regions. An experimental apparatus that confirms the conclusions reached in this cycle is recommended.*

Keywords: *Thermal development, bifurcations, viscosity*

1. INTRODUCTION

In Amado et al, 2019a, the region of flow development in bifurcations was verified with the flow of biodiesel, edible, hydraulic and lubricant oils. The correlations postulated in Amado et al, 2018, were tested there and it was concluded that Eq. (1), that verifies the effect of the variation of flow rate Q, in the region in evidence, was the expression that was best suited. This conclusion is obviously supported by the fact that the Reynolds Number, Re, is part of the variables that influence the length L of the flow development. In this way, varying the fluid means varying the viscosity and, consequently, change Re, just as varying the flow rate also results in varying Re. Thus, that correlation should be the one that would be best suited.

$$L = 0.23(2R)^{-0.1} Re^{-0.24} D^{1.1} \tag{1}$$

In this equation, R is the radius of curvature determined by the arc that contains the feeder channel and the outlet and D is the diameter of the tube that makes up the bifurcation.

According to Ghobadi. and Muzychka, 2016, in their work called "A Review of Heat Transfer and Pressure Drop Correlations for Laminar Flow in Curved Circular Ducts", until the date of publication of that paper, very little had been announced in terms of thermal developing region. So, present authors are dealing with something not yet fully understood.

The equations proposed by Amado et al, 2019b, for predicting the length of the thermal developing region L_{th}, are shown below. When there is a variation in flow rate between 5.56 x 10^{-11} m^3/s to 2.78 x 10^{-10} m^3/s, with constant half angles θ_1 *and* θ_2 as 45º and 30º and channel diameter of 0.02m, it applies the Eq (2). When there is variation of pipe diameter between 0.01 and 0.035m, with constant flow rate value (1.39 x 10^{-10} m/s) and half angles (θ_1 and θ_2 as 45º and 30º), Eq. (3) is applicable. Finally, when there is a variation of angles θ_1 and θ_2, with pairs between 5º and 90º, with constant flow rate value (1.39 x 10^{-10} m^3/s) and constant channel diameter of 0.02m, Eq. (4) is the indicated.

$$L_{th} = \frac{3.3x1^{\ -8} + 6.4x10^{-8} De^{0.5} Pr^{0.25}}{1 + 0.0122 DePr} Pr \tag{2}$$

$$L_{th} = \frac{1.8x10^{-8}+6.4x10^{-8}De^{0.5}Pr^{0.25}}{0.25+0.0488DePr}Pr \quad (3)$$

$$L_{th} = \frac{0.00035Pr^{0.2}}{De^{-0.04}} \quad (4)$$

In all cases, *De* is the Dean Number and *Pr*, the Prandtl Number.

As a broad correlation, that is, when angles, flow rates and diameters were varied at the same time, Eq. (2) was the one that best performed.

Before these equations, Janssen and Hoogendoorn, 1978, Yao, 1984, and Liu and Masliyah, 1994, presented equations that intended to predict the L_{th} extension, for flow in toroidal and helical tubes, which served as the basis for the work of Amado et al, 2019b, in bifurcations.

That said, the objective of this manuscript is established: To test the equations proposed by Amado et al, 2019b, in the same oils used in Amado et al, 2019a, and to qualitatively analyze the region of thermal development in bifurcations with angles θ_1 and θ_2, in constant pair of 30º and 45º, flow rate of 1.6 x 10^{-4} m^3/s and channel diameter of 0.02m.

2. MATERIALS AND METHODS

As performed in previous works (Amado et al, 2017, Amado et al 2018a, b, c and Amado et al 2019a, b), computer simulations using an ANSYS commercial code, student version, as well as using a handcrafted code (an in house code) were carried out with boundary conditions as established:

- Initial velocity at the inlet according to Eq. (5), where *Q* is the fluid flow rate, *a* is the radius of the channel and *r* is the distance from the central axis to the node to be calculated;

$$v_{axial} = \frac{2Q}{\pi r^4}(a^2 - r^2) \pm \cos\theta_i \quad (5)$$

- Flow rate of oils at 1,6 x 10^{-4} m^3/s, 80 ºC and under atmospheric pressure
- Velocity equal to zero near the inner wall;
- Constant heat flow through walls;
- Constant peripheral temperature at the wall;
- The flow simulated a horizontal process, that is, the action of gravity was neglected;

The physical properties were treated according to the following premises:

a) Oils flowing internally presents a convection coefficient of 2.5 W/m2K;
b) The external environment is filled with air at rest, with a convection coefficient of 1.2 W / m2K;
c) Viscosity was that provided in catalogs, usually measured at 40 ºC;
d) Density reported in the catalogs was considered compatible for viscosity temperature and Reynolds Number calculation;
e) When the catalog provided only the values of kinematic viscosity (case of hydraulic oils), the average density of 878 kg/m^3 was adopted as the standard;

See Tab. 1 to 4 with the physical properties of the different oil sets and the calculated Reynolds Number. Considering that the flow temperature and the external one are constant and respectively 80 ºC and 24 ºC, the variation of the properties "viscosity" and "density" with the temperature were not taken into account. Furthermore, they were established as constant at 40 ºC, according to values informed in the product catalogs (see letters c and d above). This premise was adopted so that the variation in the length of the region of interest could be seen depending on the type of fluid employed and not depending on the variation in viscosity and density of the same fluid. For the purpose of mathematical simplification, the authors also consider that the temperature gradient generated between the center of the tube and its internal wall was not sufficient to vary these properties in such a way that they could have an important influence on the flow velocity.

Table 1. Physical properties of biodiesel oils

Outlet	Oil type	Viscosity 40 ºC (kg/ms)	Density	Reynolds Number
Left 1	Conventional Diesel	0.00550208	859.7	795.77
Right1	Conventional Diesel	0.00550208	859.7	795.77
Left 2	Castor Biodiesel	0.00525000	875.0	848.83
Right 2	Castor Biodiesel	0.00525000	875.0	848.83
Left 3	Babassu Biodiesel	0.00449800	865.0	979.42
Right 3	Babassu Biodiesel	0.00449800	865.0	979.42
Left 4	Piqui Biodiesel	0.00345735	886.5	1305.89
Right 4	Piqui Biodiesel	0.00345735	886.5	1305.89
Left 5	Cotton Biodiesel	0.00296870	960.0	1646.93
Right 5	Cotton Biodiesel	0.00296870	960.0	1646.93
Left 6	Palm Biodiesel	0.00258309	849.7	1675.31
Right 6	Palm Biodiesel	0.00258309	849.7	1675.31

Table 2. Physical properties of edible oils

Outlet	Oil type	Viscosity 40 ºC (kg/ms)	Density (kg/m^3)	Reynolds Number
Left 7	Avocado	0.00442042	873.6	1006.51
Right 7	Avocado	0.00442042	873.6	1006.51
Left 8	Sunflower	0.00390320	873.2	1139.37
Right 8	Sunflower	0.00390320	873.2	1139.37
Left 9	Soy	0.00382539	879.4	1170.79
Right 9	Soy	0.00382539	879.4	1170.79
Left 10	Cotton	0.00369643	871.8	1201.17
Right 10	Cotton	0.00369643	871.8	1201.17
Left 11	Canola	0.00357979	877.4	1248.27
Right 11	Canola	0.00357979	877.4	1248.27

Table 3. Physical properties of hydraulic oils

Outlet	Oil type	Viscosity 40 ºC (kg/ms)	Density (kg/m^3)	Reynolds Number
Left 20	ISO VG 10	0.00878000	average value of 878.0	509.30
Right 20	ISO VG 10	0.00878000		509.30
Left 21	ISO VG 7	0.00597040		748.96
Right 21	ISO VG 7	0.00597040		748.96
Left 22	ISO VG 5	0.00403880		1107.16
Right 22	ISO VG 5	0.00403880		1107.16
Left 23	ISO VG 3	0.00289740		1543.32
Right 23	ISO VG 3	0.00289740		1543.32
Left 24	ISO VG 2	0.00193160		2314.98
Right 24	ISO VG 2	0.00193160		2314.98
Left 25	ISO VG S	0.00131700		3395.31
Right 25	ISO VG S	0.00131700		3395.31

Table 4. Physical properties of lubricant oils

Outlet	Oil type	Viscosity 40 ºC (kg/ms)	Density (kg/m^3)	Reynolds Number
Left 12	SAE 60	0.0037000	154.17	212.21
Right12	SAE 60	0.0037000	154.17	212.21
Left 13	SAE 50	0.0037000	193.71	266.64
Right 13	SAE 50	0.0037000	193.71	266.64
Left 14	SAE 40'	0.0037000	256.94	353.67
Right 14	SAE 40'	0.0037000	256.94	353.67
Left 15	SAE 40	0.0029000	201.39	353.68
Right 15	SAE 40	0.0029000	201.39	353.68
Left 16	SAE 30	0.0029000	266.06	467.25
Right 16	SAE 30	0.0029000	266.06	467.25
Left 17	SAE 20	0.0026000	348.99	683.61
Right 17	SAE 20	0.0026000	348.99	683.61

Computer simulations were performed using structured programming and finite difference discretization. The Navier-Stokes and Energy equations, which govern the phenomenon, were taken in two dimensions, according to the modus operandi adopted in the reference Amado et al, 2020, also presented to the present congress.

3. RESULTS AND DISCUSSION

Fig. 1 shows the flow developing region (a) and also the thermal developing region (b) in a standard fork (according to data initially informed), with the flow of conventional diesel, which has the properties shown in the first line of the Tab. 1.

In Fig. 1, analyzing image (b) in comparison to image (a), it can be seen that the thermal developing region has similar morphology and length to the flow developing region, for the evidenced oil. This is to be expected, since the energy equation, which determines the temperature profile, employs the information from the velocity field determined by the moment equations, to calculate the temperature gradient. In the area where there is a vortex formation, indicated in the image (a), there is an equivalent area in the thermal profile, where the temperature drops to lower levels (indicated in yellow). Apparently, the fluid's vorticity helps to cool it, making the coldest regions evident.

For oils of higher viscosity, such as the hydraulic ISO VG 10, the region of thermal development is more homogeneous. Fig. 2 shows the image (a) with the flow developing region with a shape within the pattern of the other fluids, but a more homogeneous thermal region (b). It shows only a small area in yellow, which indicates a little more cooling in the outermost part of the fork, especially in the outlet at 45º. Therefore, viscosity is shown to be a factor of thermal homogeneity, as evidenced in Amado et al, 2016.

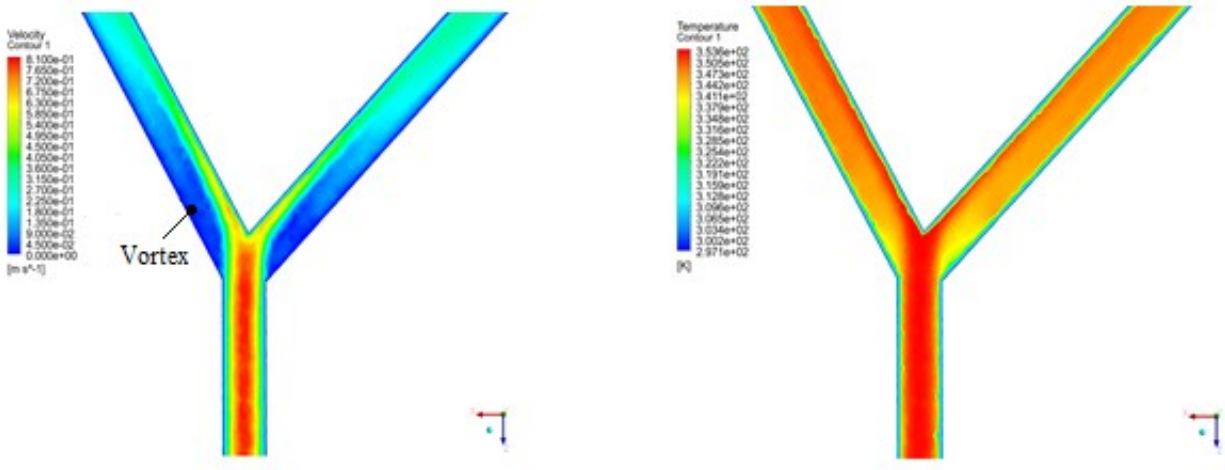

(a) (b)

Figure 1. Flow of conventional diesel at the standard bifurcation, showing (a) flow development with vortex region and (b) thermal development.

In both Fig. 1 and 2, it can be noted that the thermal developing region is much longer than those presented in Amado et al 2019b. It turns out that in that work and its predecessors, the flow rate used was quite low (1.39 x 10^{-10} m^3/s), since

it was intended to be compared with the flow in microchannel forks. However, in the present manuscript, the flow rate is considerably higher (1.6 x 10^{-4} m^3/s), closer to the limit of *Re* values for laminar flow.

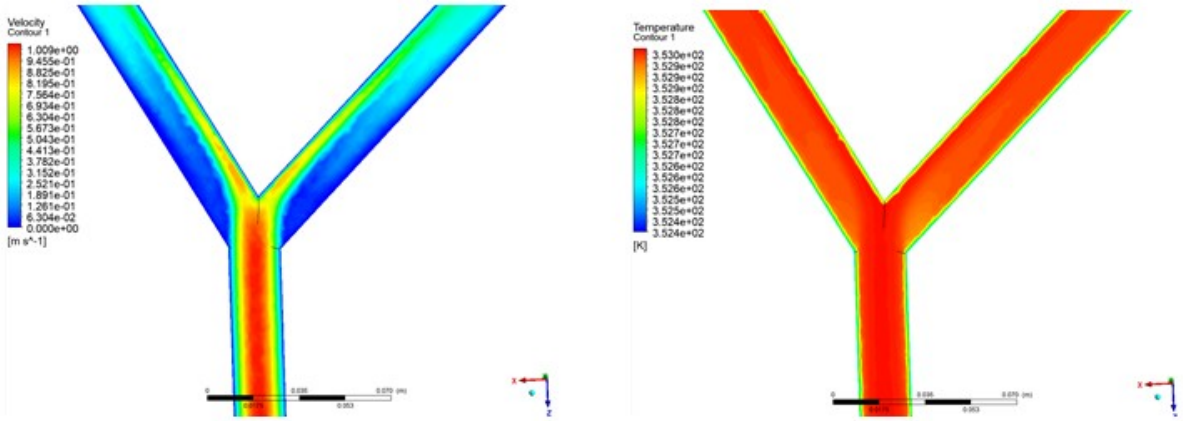

(a) (b)

Figure 2. Flow of ISO VG 10 hydraulic oil at the standard fork, showing (a) the flow development region and (b) the thermal development region.

Measurements of the thermal developing region length L_{th} are presented in Tab. 5 to 8, third column.

Figures 3 and 4 show the behavior of the thermal developing regions, respectively for the outlets at 30º and 45º.

Both in Tables 5 to 8 and in Figures 3 and 4, it can be seen that the lowest Reynolds Number values, which resulted from the combination of the low values of viscosity and density, presented the lowest measured values of L_{th}. It is also important to highlight that the measured L_{th} values from *Re* equal to 467.25 onwards have become practically constant, that is, there is an asymptotic behavior towards 0.096 m for the outlet at 30º and towards 0.0672 for the outlet at 45º. This fact shows that the region of interest is much more sensitive to dimensional characteristics than to physical properties. Additionally, in Amado et al 2016, it is shown that viscosity is an insulating property and therefore a temperature stabilizing factor.

When comparing L_{th} for the variation of the half-angles (outlets on the left and on the right), it can be noted that between 30º and 45º there is a considerable difference in the values (about 50%). Although the present manuscript is restricted only to the two half-angles of the standard asymmetric fork, these results confirm the conclusions reached in Amado et al, 2019a, where it is shown that the greater the half-angle, the greater the region of thermal development.

If L_{th} is calculated using Eq. (2) to (4), proposed by Amado et al, 2019a, there will be no good coincidence. The fact is that the flow rates employed herein were higher than those worked in the reference. Thus, from the present measurements, Eq. (6) was the one that best suited.

$$L_{th} = \frac{0.038Pr^{0.2}}{De^{-0.04}} \tag{6}$$

This correlation implies the results presented in the last column of Tables 5 to 8, with a maximum error of about 10%. It joins the list of correlations raised by the author over the past 3 years and can be useful in better understanding the behavior of the flow through the bifurcations, as well as in their dimensioning.

That said, it is important to show that an experimental apparatus is in the design phase, in the sense of giving laboratory confirmation to the conclusions reached in the present manuscript and endorsement to the advancement of the state of the art of the matter. Experimental surveys are urgent in confirming all the correlations raised by the author throughout his work to better understand the fluid dynamics that happens within bifurcated structures.

Table 5. Thermal length measurements and calculated for biodiesel oils

Outlet	Oil type	Reynolds Number	L_{th} measured (m)	L_{th} calculated (m)
Left 1	Conventional Diesel	795.77	0.0960	0.086296
Right1	Conventional Diesel	795.77	0.0672	0.087707
Left 2	Castor Biodiesel	848.83	0.0960	0.085638
Right 2	Castor Biodiesel	848.83	0.0672	0.087038
Left 3	Babassu Biodiesel	979.42	0.0960	0.083348
Right 3	Babassu Biodiesel	979.42	0.0672	0.084711
Left 4	Piqui Biodiesel	1305.89	0.0960	0.079684
Right 4	Piqui Biodiesel	1305.89	0.0672	0.080987
Left 5	Cotton Biodiesel	1646.93	0.0960	0.077772
Right 5	Cotton Biodiesel	1646.93	0.0672	0.079044
Left 6	Palm Biodiesel	1675.31	0.0960	0.075672
Right 6	Palm Biodiesel	1675.31	0.0672	0.076910

Table 6. Thermal length measurements and calculated for edible oils

Outlet	Oil type	Reynolds Number	L_{th} measured (m)	L_{th} calculated (m)
Left 7	Avocado	1006.51	0.0960	0.085838
Right 7	Avocado	1006.51	0.0672	0.087241
Left 8	Sunflower	1139.37	0.0960	0.082495
Right 8	Sunflower	1139.37	0.0672	0.083844
Left 9	Soy	1170.79	0.0960	0.083728
Right 9	Soy	1170.79	0.0672	0.085097
Left 10	Cotton	1201.17	0.0960	0.083213
Right 10	Cotton	1201.17	0.0672	0.084574
Left 11	Canola	1248.27	0.0960	0.082766
Right 11	Canola	1248.27	0.0672	0.084119

Table 7. Thermal length measurements and calculated for hydraulic oils

Outlet	Oil type	Reynolds Number	L_{th} measured (m)	L_{th} calculated (m)
Left 12	ISO VG 10	509.30	0.0672	0.095000
Right12	ISO VG 10	509.30	0.0950	0.096553
Left 13	ISO VG 7	748.96	0.0672	0.088857
Right 13	ISO VG 7	748.96	0.0950	0.090310
Left 14	ISO VG 5	1107.16	0.0672	0.083036
Right 14	ISO VG 5	1107.16	0.0950	0.084394
Left 15	ISO VG 3	1543.32	0.0672	0.078391
Right 15	ISO VG 3	1543.32	0.0950	0.079672
Left 16	ISO VG 2	2314.98	0.0672	0.073070
Right 16	ISO VG 2	2314.98	0.0950	0.074265
Left 17	ISO VG S	3395.31	0.0672	0.068377
Right 17	ISO VG S	3395.31	0.0672	0.069495

Table 8. Thermal length measurements and calculated for lubricating oils

Outlet	Oil type	Reynolds Number	L_{th} measured (m)	L_{th} calculated (m)
Left 20	SAE 60	212.21	0.08947	0.089012
Right 20	SAE 60	212.21	0.06660	0.090467
Left 21	SAE 50	266.64	0.09188	0.089556
Right 21	SAE 50	266.64	0.06700	0.091020
Left 22	SAE 40'	353.67	0.09860	0.090233
Right 22	SAE 40'	353.67	0.06716	0.091708
Left 23	SAE 40	353.68	0.09820	0.085942
Right 23	SAE 40	353.68	0.06720	0.087347
Left 24	SAE 30	467.25	0.09700	0.086582
Right 24	SAE 30	467.25	0.06720	0.087998
Left 25	SAE 20	683.61	0.09700	0.085576
Right 25	SAE 20	683.61	0.06720	0.086975

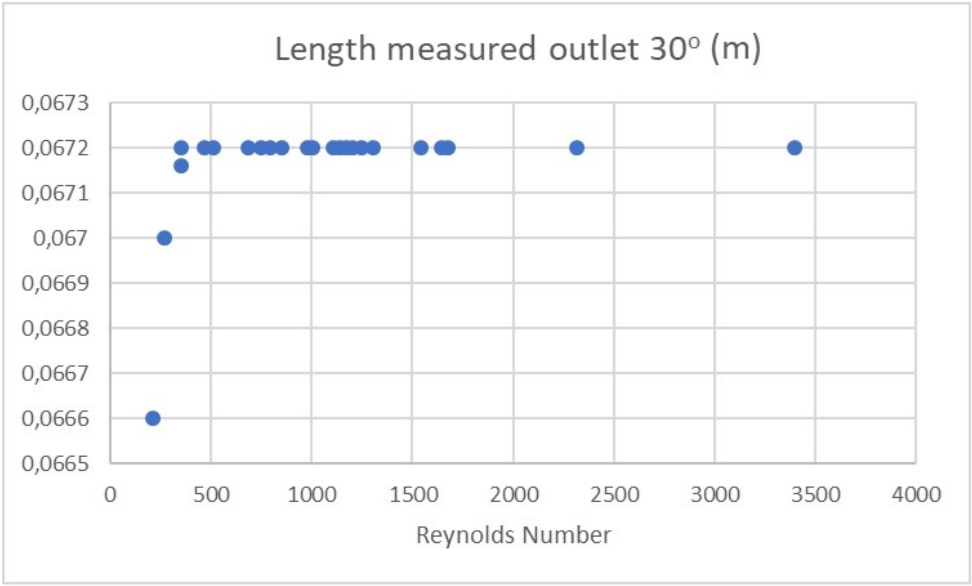

Figure 3. Measured values of L_{th} for the half-angle 30º

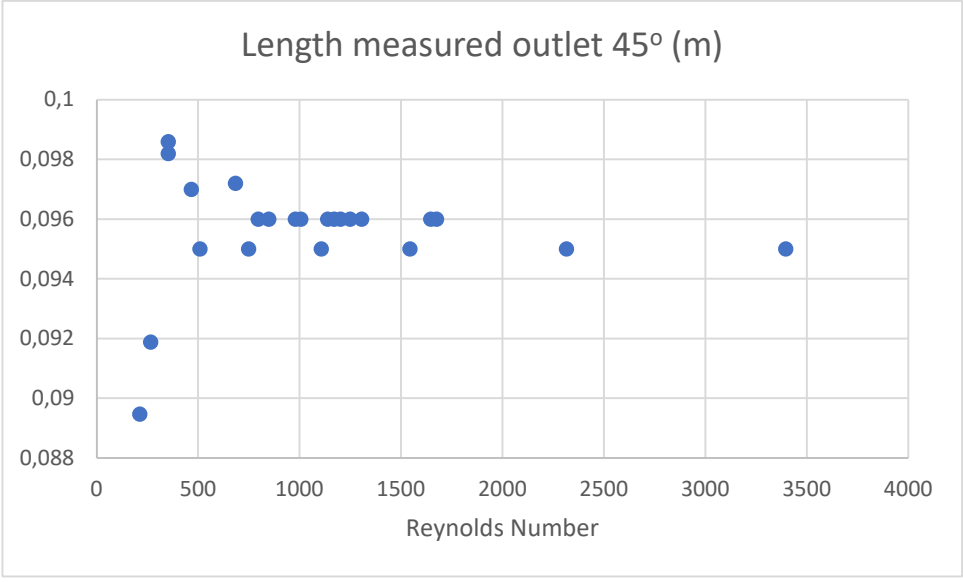

Figure 4. Measured values of L_{th} for the half-angle 45º

4. CONCLUSIONS

The region of thermal development in bifurcations, with internal flow of four oil families (biodiesels, edibles, hydraulics and lubricants) was analyzed. It was observed that its morphological aspect is similar to that of the flow developing region and that the proportionality relations regarding half angles, flow rates and channel diameters are kept.

The equations established in the authors' previous works, as well as those found in the related literature, were not successful in predicting the extension of the thermal developing region, L_{th}. In this way, from computer simulations and measurements made on images resulting therefrom, it was possible to raise the correlation $L_{th} = \frac{0{,}038Pr^{0.2}}{De^{-0.04}}$, which foresees such lengths in good coincidence bifurcations with thermal flows within the Reynolds Number universe from 509.30 onwards, with fixed half-angles at 30º and 45º, flow rates of $1.6\text{x}10^{-4}$ m^3/s and channel diameter of 0.20 m.

This work completes a series of papers by the author and collaborators regarding the regions of flow and thermal development. It is recommended to build an experimental apparatus that corroborates the conclusions established in such previous works, as well as in the present manuscript.

5. ACKNOWLEDGEMENTS

The authors acknowledge “Programa Pesquisa Produtividade - Universidade Estácio de Sá” for funding the research.

6. REFERENCES

Amado, F. P., 2020, “Critical Reynolds Number in Bifurcations*”, to be publiched in the proceedins of the 18th Brazilian Congress of Thermal Sciences and Engineering - ENCIT 2020*, November 16-20, 2020, Bento Gonçalves, RS, Brazil

Amado, F. P., Avelino, M. R., Lucena, E. S., Colman, J., 2017, “The Region of not Fully Developed Flow in Bifurcations of Microchannels” *Abstract in the proceedings of the IX Seminário de Pesquisa da Estácio e V Jornada de Iniciação Científica da UNESA*, Rio de Janeiro, Brazil.

Amado, F. P., Avelino, M. R., Lucena, E. S., Colman, J., Mazzarela, N. G. S., 2018a, “Developing Flow in the Inlet Region of Bifurcations in Microchannels with Symmetric Angulation”, *in the Proceedings of the X Congresso Brasileiro de Engenharia Mecânica - CONEM 2018*, Salvador, BA, Brazil, 2018; DOI: 10 26678/ABCM CONEM2018 CON18-0253.

Amado, F. P., Avelino, M. R., Lucena, E. S., Colman, J., Mazzarela, N. G. S., 2019a, “Forecasting the Length of the Thermal Developing Region at the Entrance of Bifurcations”, *in the proceedings of the 25th ABCM International Congress of Mechanical Engineering - COBEM 2019*, Vol. 1, Uberlândia, MG, Brazil. DOI://10.26678/ABCM.COBEM2019.COB2019-0044

Amado, F. P., Avelino, M. R., Lucena, E. S., Colman, J., Mazzarela, N. G. S., 2018b, “Forecasting the Length of the Undeveloped Flow Region in the Inlet of Asymmetric Bifurcations I*”, in the Proceedings of the 17th Brazilian Congress of Thermal Sciences and Engineering - ENCIT 2018*, Águas de Lindóia, SP, Brazil,; DOI: 10 26678/ABCM ENCIT2018 CIT18-0008

Amado, F. P., Avelino, M. R., Lucena, E. S., Colman, J., Mazzarela, N. G. S., 2018c, “Forecasting the Length of the Undeveloped Flow Region in the Inlet of Asymmetric Bifurcations II”, *in the Proceedings of the 17th Brazilian Congress of Thermal Sciences and Engineering - ENCIT 2018*, Águas de Lindóia, SP, Brazil,; DOI: 10 26678/ABCM ENCIT2018 CIT18-0009

Amado F. P., Corradi, V. H. M., Vergara, P. H., Silva, W. A., Mazzarela, N. G. S., 2019b, “Influence of Low Reynolds Number in the Region of Flow Development in Bifurcations”, *in the Proceedings of the 25th ABCM International Congress of Mechanical Engineering - COBEM 2019*, Uberlândia, MG, Brazil. DOI://10.26678/ABCM.COBEM2019.COB2019-0012

Amado F. P., Lucena, E. S., Avelino, M. R., 2016, “Behavior of temperature gradients in fuel oil exportation through a 12 inches pipe under inviscid and viscous conditions*”, in the proceedings of IX Congresso Nacional de Engenharia Mecânica - CONEM 2016*, Fortaleza, Ceará, Brazil; DOI:10.20906/CPS/CON-2016-0026

Ghobadi. M., Muzychka, Y. S., 2016, “A Review of Heat Transfer and Pressure Drop Correlations for Laminar Flow in Curved Circular Ducts”, *Heat Transfer Engineering*, 37:10, 815-839, DOI: 10.1080/01457632.2015.1089735.

Janssen, L. A. M., and Hoogendoorn, C. J., 1978. “Laminar Convection Heat Transfer in Helical Coiled Tubes”. *International Journal of Heat and Mass Transfer*, vol. 21, pp.1197–1206;

Liu, S., and Masliyah, J. H., 1994. "Developing Convective Heat Transfer in Helical Pipes With Finite Pitch". *International Journal of Heat and Fluid Flow*, vol. 15, no. 1, pp. 66–75;

Yao, L. S., 1984. "Heat Convection in a Horizontal Curved Pipe", *Journal of Heat Transfer*, vol. 106, pp. 71–77.

7. RESPONSIBILITY NOTICE

The authors are the only responsible for the printed material included in this paper.